Multiphase Flow through a Granular Material under Hydro-Mechanical Loading

Rana AL NEMER, Giulio SCIARRA, Julien RÉTHORÉ

Nantes Université, Ecole Centrale Nantes, CNRS, GeM, UMR 6183

Context, Problematic & Objectives

Context

Underground storage of energies (H_2, CH_4) in geological formations; CO_2 sequestration, Radioactive waste disposal...

[Hefny *et al.*, 2020]

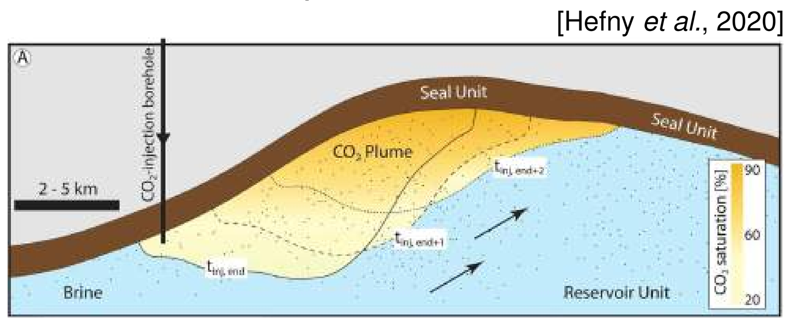

Problematic

Infiltration of gas into the sealing rock via pre-existing cracks / formation of new pathways, in the form of **fingered patterns**

[Adapted from: Kivi *et al.*, 2022]

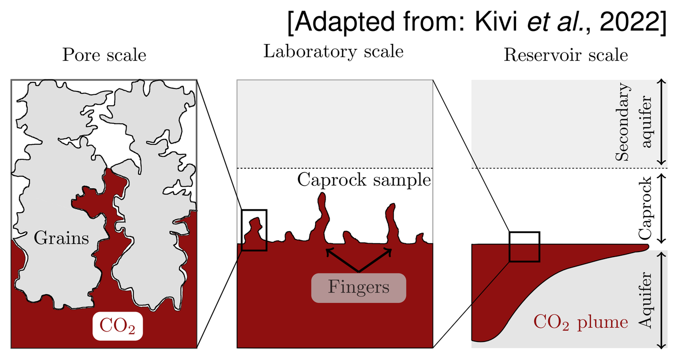

Objectives

- Investigate the effect of **unstable gas infiltration** on the **mechanical response** of the porous skeleton
- Investigate the effect of **mechanical loading** on the **skeleton response** and **bi-phasic flow**

Literature example with Hele-Shaw cell

Weak points:

- Unstable pattern issued from a **point-wise** injection
- **Absence** of mechanical loading
- Glass beads **not** ideal for imaging and DIC

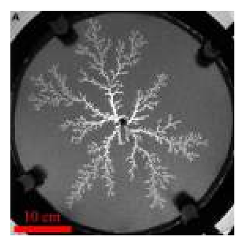

Two-Phase flow (Air-Water)

Volumetric strain by DIC

[Eriksen *et al.*, 2015]

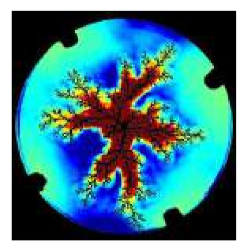

Experimental means

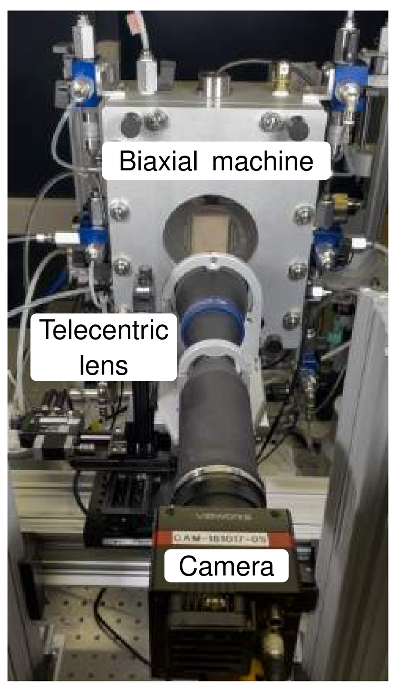

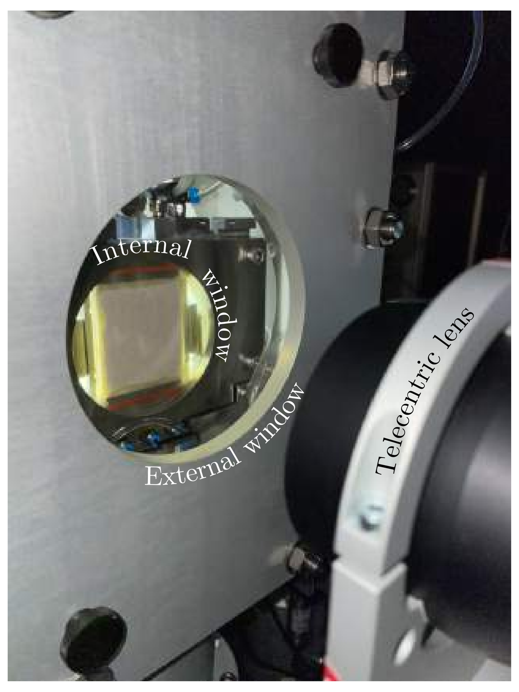

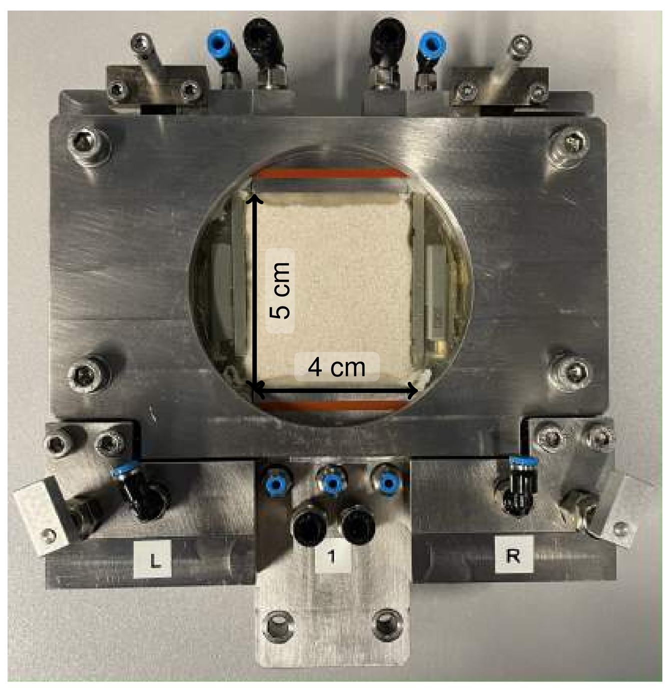

Biaxial machine with hydro-mechanical control

- Simultaneous control of confining and three fluid pressures (Maximum pressure = 1600 kPa)
- Particular system for transmitting the confining pressure to the lateral borders of the sample
- Sample cell enclosing a specimen of $(4 \times 5 \times 1.1)$ cm^3 filled by **Fontainebleau sand NE34**

High-resolution optical system

- Camera of 50 MPx & Spatial resolution of 6.1 µm/pixel (1 grain of FB ≈ (25-50) pixels)
- Maximum acquisition frequency = 30 Hz

Drainage test procedure:

1. Initial confining pressure 50 kPa
2. Saturation with deaerated water
3. Skempton approach for full saturation: sequence of stepwise increments of Confining pressure P_{conf} & Pore water pressure P_w [Head *et al.*, 1998]
4. Adjustment of effective stress to the desired value σ'_0
5. Induced-drainage by controlling the air pressure P_a ($P_a > P_w$)

[Al Nemer *et al.*, 2022]

Results — Air infiltration through water-saturated sand

Test (1): $P_{cap} = P_a - P_w = 30$ kPa & $\sigma'_0 = P_{conf} - P_w = 120$ kPa → **Single** localized infiltration

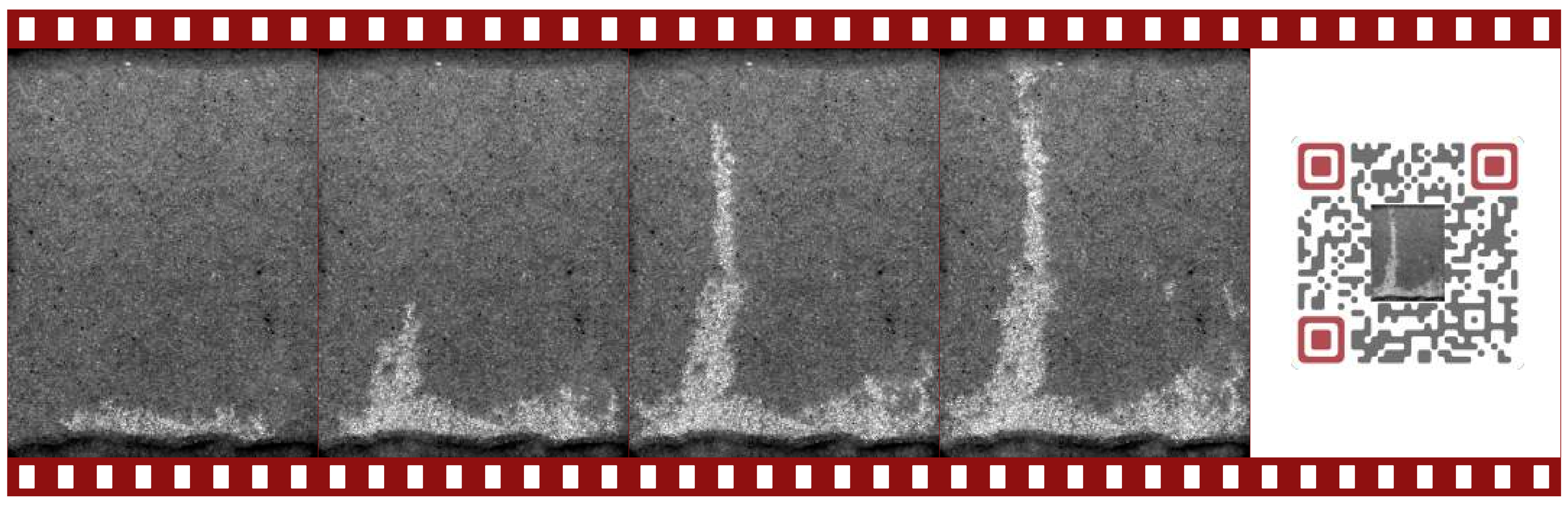

Frame 8 | 20 | 34 | 48 | Video

Test (2): $P_{cap} = P_a - P_w = 30$ kPa & $\sigma'_0 = P_{conf} - P_w = 40$ kPa → **Double** localized infiltration

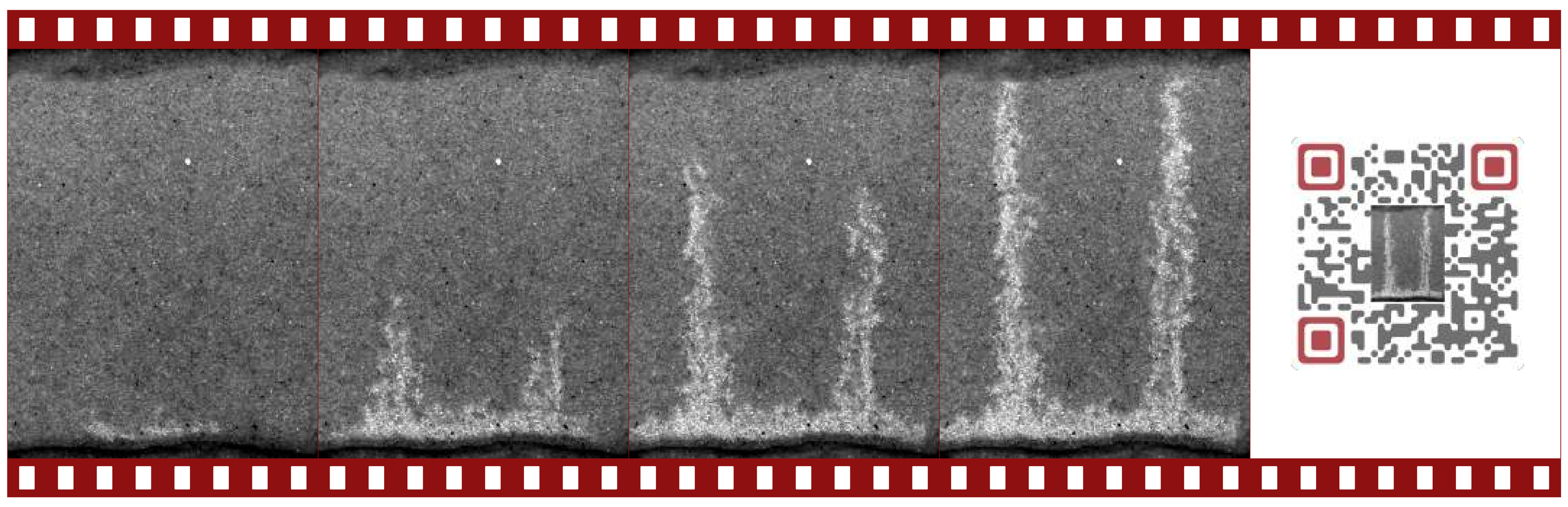

Frame 5 | 13 | 21 | 29 | Video

Results — Mechanical loading & Strain localization

Volumetric strain maps at the breakthrough time*

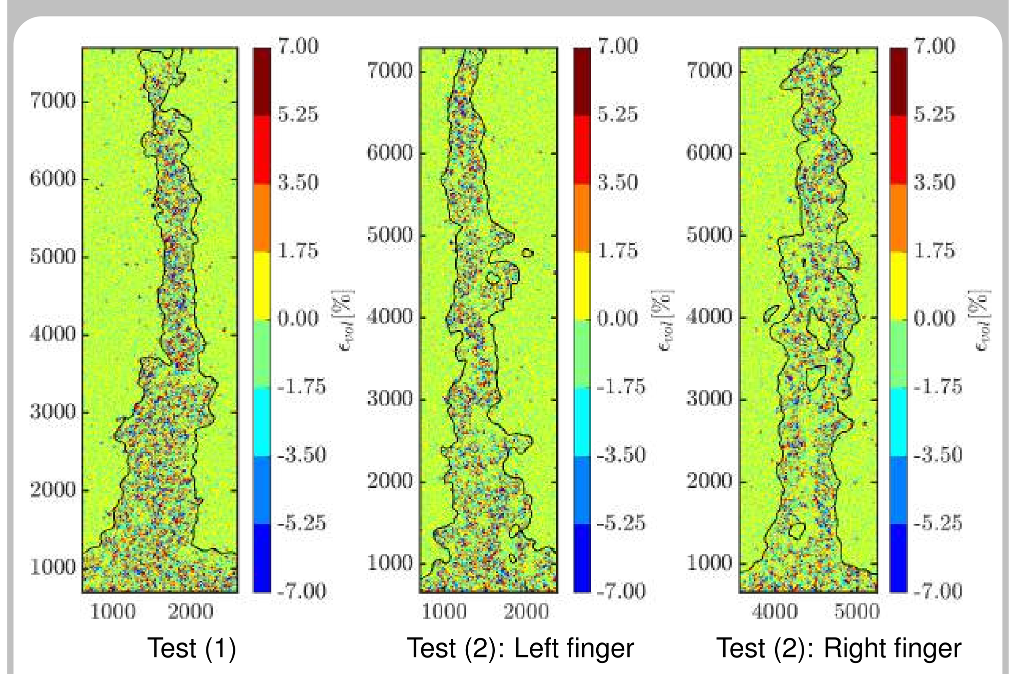

- Volumetric strains calculated by FE-DIC [Réthoré, 2018]
- Bi-phasic flow induces localized strains
- Local strains: $\epsilon_{vol} > 0$: Dilation & $\epsilon_{vol} < 0$: Compaction
- Dense distribution in (1) vs. hollow distribution in both fingers of (2): $\nearrow \sigma'_0 \Rightarrow$ more new paths are opened

* Breakthrough time is the time at which the air reaches the top of the sample.

Volumetric strains averaged within the developed finger along the drainage process

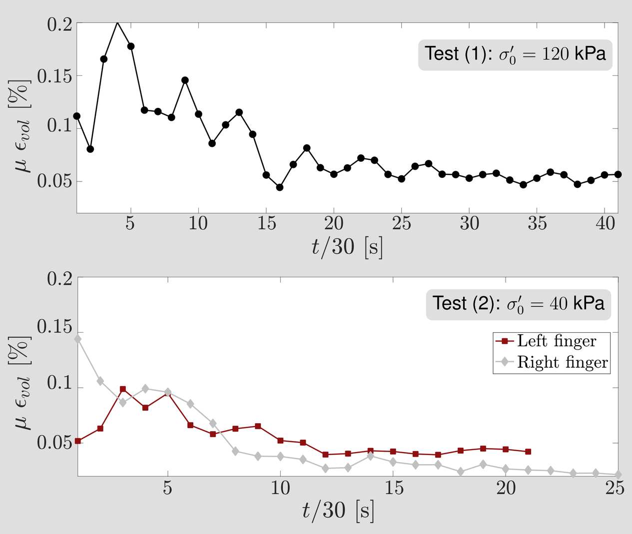

- $\mu\ \epsilon_{vol} > 0$: Dilation of the medium
- $\mu\ \epsilon_{vol_{(1)}} > \mu\ \epsilon_{vol_{(2)}}$: $\nearrow \sigma'_0 \Rightarrow \nearrow$ Global average strain

Transition zones* through the drainage process

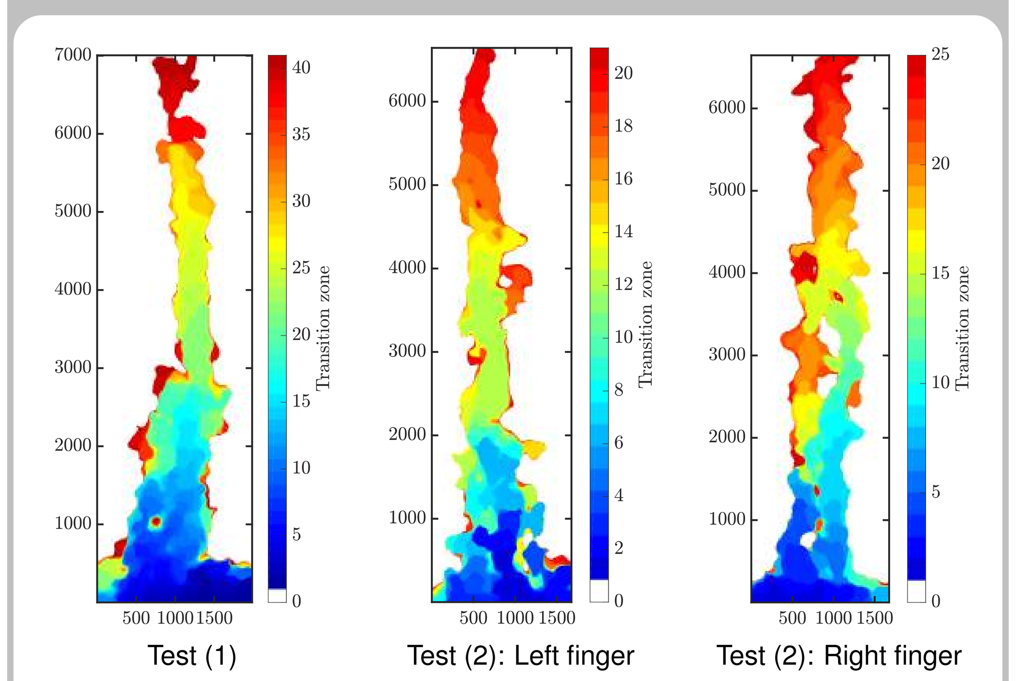

* Transition zones are consecutive surfaces invaded by the injected air.

Volumetric strains at the breakthrough time averaged within the transition zones

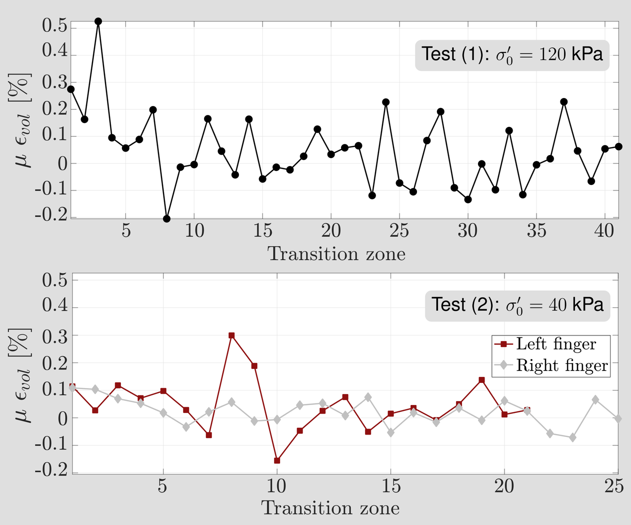

- Base of the finger is always described by a positive average strain: Opening of the medium
- Deformed area is a series of compacted and dilated zones
- $\nearrow \sigma'_0 \Rightarrow \nearrow$ Local average strain

Results — Mechanical loading & Bi-phasic interface

Growth property: Invaded area

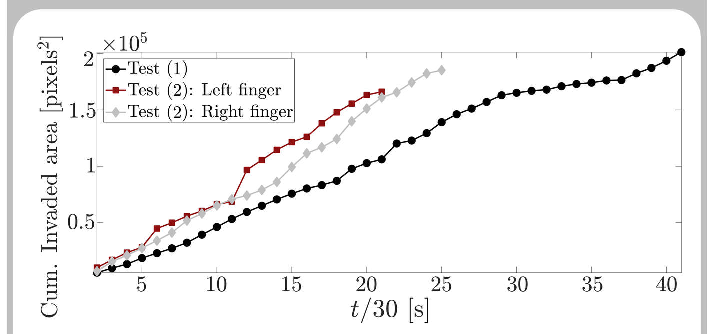

- $\nearrow \sigma'_0 \Rightarrow$ Smaller transition zone area
- $\nearrow \sigma'_0 \Rightarrow$ Larger drained zone

The detected interface, in this whole analysis, is determined by a customized robust algorithm based on the Mumford-Shah functional for segmentation analysis. [Mumford and Shah, 1989]

Morphological property: Corrugation amplitude

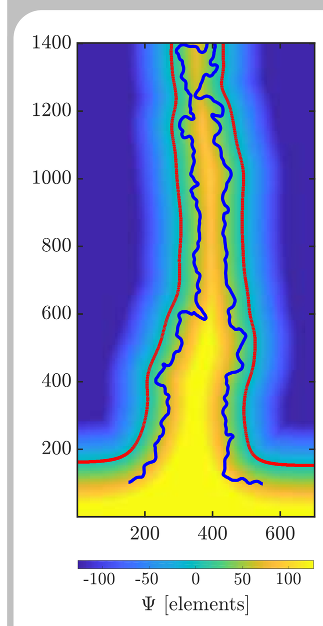

Test (1)

Corrugation amplitude $\mathcal{A}$ is determined as the standard deviation of the signed distance Ψ between a smooth reference interface (in red) and an ondulated one (in blue). [Brouzet *et al.*, 2021]

Finger	$\mathcal{A}$ [pixels] (Left - Right) borders
(1)	57-52
(2) Left	45-74
(2) Right	58-56

Interface **topology** is not affected by the mechanical loading, but rather by the **microstructure** of the medium.

Conclusions

- Unstable infiltration generates localized strains within the developed finger and induces an opening of the granular medium.
- The mechanical loading influences the preferential pathways of the injected fluid: the higher the applied effective stress is, the more local the percolation will be.
- The mechanical loading also influences the magnitude of the induced strains: the higher the applied effective stress is, the higher the strains will be.
- The mechanical loading has no influence on the interface morphology but rather on its growth.

Contact

Rana AL NEMER (rana.al-nemer@ec-nantes.fr); Giulio SCIARRA (Giulio.Sciarra@ec-nantes.fr); Julien RÉTHORÉ (julien.rethore@ec-nantes.fr)

Nantes Université · CENTRALE NANTES · GeM · cnrs · anr